Applied Nanoscience (2020) 10:3045–3055
https://doi.org/10.1007/s13204-019-01038-w

ORIGINAL ARTICLE

Computational analysis of entropy generation for cross-nanofluid flow

M. Ali[1] · W. A. Khan[2,3] · M. Irfan[4] · F. Sultan[1] · M. Shahzed[1] · M. Khan[4]

Received: 19 January 2019 / Accepted: 9 April 2019 / Published online: 20 April 2019

Abstract
This research work is made to demonstrate diverse characteristics of entropy generation minimization for cross nanomaterial towards a stretched surface in the presence of Lorentz's forces. Transportation of heat is analyzed through Joule heating and radiation. Nanoliquid model consists of activation energy and Brownian movement aspects. Concentration of cross material is scrutinized by implementing zero mass flux condition. Bejan number and entropy generation (EG) rate are formulated. The employment of transformation variables reduces the PDEs into nonlinear ODEs. Bvp4c scheme is implemented to compute the computational results of nonlinear system. Velocity, temperature, and concentration are conducted for cross nanomaterial. Consequences of current physical model are presented through graphical data and in tabular form. The outcomes for Bejan number and EG rates are presented through graphical data. It is noted that EG rates and Bejan number significantly affect rate of heat-mass transport mechanisms. In addition, graphical analysis reveals that E.G. rate has diminishing trend for diffusive variable. Moreover, achieved data reveal that profiles of Bejan number boost for augmented values of radiation parameter.

Keywords Cross nanoliquid · Thermal radiation · Entropy generation · Activation energy

Introduction

The advancement in nanotechnology and nanoscience extended the application areas for researchers and scientists. Applications of nanofluids are encouraging in different phenomena such as the heat transfer phenomena. Advancements in technology need the proficient methods for heat transfer, and nanofluids provide the more efficient medium for heat transfer from one source to another source. In addition, numerous procedures are available in the literature which can intensifies heat transport properties in flow to improve the effectiveness of concentrating collector. Nanoliquids have higher thermo-physical properties compared with those of base liquids. Moreover, nanoliquids were employed inside absorber to serve as heat transfer liquid and, therefore, boost the performance of solar system. Sheikholeslami et al. (2014) deliberated the flow for CuO water nanofluid by considering the aspects of Lorentz forces. Khan et al. (2014) described heat sink–source characteristics for 3D non-Newtonian nanofluid. Ellahi et al. (2015) inspected the colloidal analysis for CO–H_2O over inverted vertical cone. Khan and Khan (2015), (2016a) and Khan et al. (2016a) described various properties of nanoliquid by considering different non-Newtonian fluid models. Waqas et al. (2016) examined the flow of micropoler liquid due to nonlinear stretched sheet with convective condition. Khan and Khan (2016b) reported features of Burgers fluid by considering nanoparticles. Sulochana et al. (2017) studied the consequences of thin din needle with Joule heating. Hayat et al. (2017) analyzed radiative heat transfer in the presence of Lorentz's force for nanofluid. Sheikholeslami and Shehzad (2017) reported the properties of nanofluid by considering characteristics of Lorentz force. Moreover, some recent development on nanofluid has been discussed in Sheikholeslami and Shamlooei (2017), Sheikholeslami and Rokni (2017), Irfan et al. (2018a, b, 2019a), Hayat et al. (2018), Sheikholeslami et al. (2018), Gireesha et al. (2018), Mahanthesh et al. (2018), Sheikholeslami (2018a, b), Akbar

✉ W. A. Khan
Waqar_qau85@yahoo.com

1 Department of Mathematics and Statistics, Hazara University, Mansehra 21300, Pakistan

2 School of Mathematics and Statistics, Beijing Institute of Technology, Beijing 100081, China

3 Department of Mathematics, Mohi-ud-Din Islamic University, Nerian Sharif 12010, Azad Jammu & Kashmir, Pakistan

4 Department of Mathematics, Quaid-I-Azam University, Islamabad 44000, Pakistan

and Khan (2016), Sheikholeslami and Shehzad (2018a, b), Sheikholeslami and Sadoughi (2018), Sheikholeslami and Seyednezhad (2018), Khan et al. (2018a), Sheikholeslami and Rokni (2018), Sheikholeslami et al. (2019a, b), Sheikholeslami (2019a, b), Khan et al. (2019), Sheikholeslami and Mahian (2019), Nematpour-Keshteli and Sheikholeslami (2019).

The mass transfer phenomena is considered as an important unit of chemical process. In these phenomena, chemically reacting species (molecules) are moving from low concentrated area to high concentration. Chemical processes plays the vital role in culture and life itself. Chemical reactions are categorized in different systems due to their chemical and physical behavior, and homogeneous and heterogeneous systems are two major systems among them. Homogeneous reactions lie in the same phase space, i.e., gas, liquid, or solid spaces, while the heterogeneous reactions required more than one phase space. Khan et al. (2016b, 2017) scrutinized features chemical mechanisms for non-Newtonian fluids. Mahanthesh et al. (2017) discovered properties of vertical cone for colloidal material. Shahzad et al. (2019) reported the properties of C-matrix by employing new mathematical concept. Features of revised relation for flux and chemical processes were considered by Sohail et al. (2017). Ramesh et al. (2018) deliberated the revised conditions at boundary utilizing Maxwell nanoliquid. Irfan et al. (2018c) considered characteristics of variable conductivity and chemical processes for Carreau fluid. Tangent hyperbolic nanofluid with aspects of chemical processes and activation energy were inspected by Khan et al. (2018b). Irfan et al. (2019b) discussed the heterogeneous–homogeneous reactions for Oldroyd-B fluid.

To our knowledge, mathematical modeling for cross nanoliquid with entropy generation minimization is not yet examined. With this point of view, our concern here is to model cross nanofluid with entropy generation. Effects of viscous dissipation and thermal radiation are reported. Nanofluid modeling comprises the thermophoretic and Brownian movement aspects. Zero mass flux-type boundary condition is imposed. Idea of activation energy (AE) along with chemical reaction is also introduced. Total EG (entropy generation) rate and Bejan number are discussed for various flow variables. Numeric solutions for nonlinear systems are constructed. Nature of emerging physical is analyzed through graphs and tables.

Technical depiction and flow field equations

Our intention here is to formulate mixed convective cross nanomaterial flow towards moving surface. Moreover, we have considered magnetic field aspects for cross nanomaterial which acts normal to surface. Transportation of heat is analyzed by considering radiation and Joule heating aspects. The innovative relation of activation energy is introduced. Moreover, zero flux condition regarding nanofluid is imposed at boundary. Keeping in view the afforested assumptions, boundary layer approximation governs the following system of equations:

$$\frac{\partial u}{\partial x}+\frac{\partial v}{\partial y}=0, \tag{1}$$

$$u\frac{\partial u}{\partial x}+v\frac{\partial u}{\partial y}=\upsilon\frac{\partial^2 u}{\partial y^2}\left[\frac{1}{1+(\Gamma\frac{\partial u}{\partial y})^n}\right]+\upsilon\frac{\partial u}{\partial y}\frac{\partial}{\partial y}\left[\frac{1}{1+(\Gamma\frac{\partial u}{\partial y})^n}\right]-\frac{\sigma\times B_0^2}{\rho_f}u+g\left[A_1\left(T-T_\infty\right)+A_2\left(C-C_\infty\right)\right] \tag{2}$$

$$u\frac{\partial T}{\partial x}+v\frac{\partial T}{\partial y}=\frac{\nu}{c_p}\left(\frac{\partial u}{\partial y}\right)^2\left[\frac{1}{1+(\Gamma\frac{\partial u}{\partial y})^n}\right]+\alpha\frac{\partial^2 T}{\partial y^2}+\tau\frac{D_T}{T_\infty}\left(\frac{\partial T}{\partial y}\right)^2+\tau D_B\frac{\partial C}{\partial y}\frac{\partial T}{\partial y}-\frac{1}{(\rho c)_f}\frac{\partial q_r}{\partial y}, \tag{3}$$

$$u\frac{\partial C}{\partial x}+v\frac{\partial C}{\partial y}+w\frac{\partial C}{\partial z}=\frac{D_T}{T_\infty}\frac{\partial^2 T}{\partial y^2}+D_B\frac{\partial^2 C}{\partial y^2}-k_r^2\left(\frac{T}{T_\infty}\right)^m\left(C-C_\infty\right)\exp\left(-\frac{E_a}{KT}\right), \tag{4}$$

with

$$u=U_{\mathrm{w}}=cx, v=0,\ T=T_{\mathrm{w}},\quad D_{\mathrm{B}}\frac{\partial C}{\partial y}+\frac{D_{\mathrm{T}}}{T_\infty}\frac{\partial T}{\partial y}=0\quad \text{at } y=0, \tag{5}$$

$$u\to 0,\ T\to T_\infty,\ C\to C_\infty \text{ as } y\to\infty. \tag{6}$$

Here, $(v,\ u)$ symbolizes velocity components in $(y,\ x)$ direction, ρ_f is the density of cross liquid, $\nu=\frac{\mu}{\rho_f}$ is the kinematic viscosity of fluid, μ is the dynamic viscosity, Γ is the material constant, B_0 is the uniform magnetic field strength, $\tau=\frac{(\rho c)_\rho}{(\rho c)_{\mathrm{f}}}$ is the ratio of heat capacity, with $(\rho c)_{\mathrm{f}}$ heat capacity of fluid and $(\rho c)_{\mathrm{p}}$ is the effective heat capacity of nanoparticles, $\alpha=\frac{k}{(\rho c)_{\mathrm{f}}}$ is the thermal diffusivity, k is the thermal conductivity of liquid, c_{p} is the specific heat capacity, σ^* is the electrical conductivity, $\left(D_{\mathrm{B}},\ D_{\mathrm{T}}\right)$ are the (Brownian and thermophoresis) diffusion coefficients, $(T,\ C)$ are the (temperature and concentration), $\left(T_\infty,\ C_\infty\right)$ are the ambient (temperature, concentration), T_{w} is the

surface temperature, k_r^2 is the reaction rate, E_a is the activation energy, m is the fitted rate constant, c is the dimensional constant, and U_w is the stretching velocity.

Considering

$$\eta = y\sqrt{\frac{c}{\nu}}, u = cxf'(\eta),\ \nu = -\sqrt{c\nu}f(\eta),\quad \theta(\eta) = \frac{T - T_\infty}{T_w - T_\infty},\ \phi(\eta) = \frac{C - C_\infty}{C_\infty}. \tag{7}$$

One has

$$\left[1 + (1-n)\left(Wef''\right)^n\right]f''' - \left[1 + \left(Wef''\right)^n\right]^2 \left[f'^2 + ff'' + \lambda\left(\theta + N_r\phi\right)\right] = 0, \tag{8}$$

$$\left(1 + \frac{4}{3}R\right)\theta'' + Pr\left[f\theta' + Nb\theta'\phi' + Nt\theta'^2 + \frac{Ecf''^2}{1 + \left(Wef''\right)^n}\right] = 0, \tag{9}$$

$$\phi'' + Sc\left[f\phi' + \frac{Nt}{Nb}\theta'' - \sigma(1+\delta\theta)^m\phi\exp\left(-\frac{E}{1+\delta\theta}\right)\right] = 0, \tag{10}$$

$$f(0) = 0,\ f'(0) = 1,\ f'(\infty) \to 0, \tag{11}$$

$$\phi'(0) = -\frac{N_t}{N_b}\theta(0),\ \theta(\infty) \to 0, \tag{12}$$

$$\phi(0) = 1,\ \phi(\infty) \to 0, \tag{13}$$

where prime $(')$ denotes differentiation with respect to η, $M = \frac{\sigma B_0^2}{\rho_f c}$ is the magnetic parameter, $\Pr = \frac{\nu}{\alpha}$ is the Prandtl number, $R = \frac{4\sigma^{**}T_\infty^3}{kk^*}$ is the thermal radiation parameter, $\mathrm{Nb} = \frac{\tau D_B C_\infty}{}$ is the Brownian motion parameter, $\mathrm{Nt} = \frac{\tau D_T\left(T_w - T_\infty\right)}{\nu T_\infty}$ is the thermophoresis parameter, $\mathrm{Ec} = \frac{c^2x^2}{c_p\left(T_w - T_\infty\right)}$ is the Eckert number, $\mathrm{We} = \sqrt{\frac{\Gamma^2c^3x^2}{\nu}}$ is the local Weissenberg number, $\mathrm{Sc} = \frac{\nu}{D_B}$ is the Schmidt number, $\sigma = \frac{kr^2}{c}$ is the dimensionless reaction rate, $E = \frac{E_a}{KT_\infty}$ is the dimensionless activation energy, and $\delta = \frac{T_w - T_\infty}{T_\infty}$ is the temperature difference parameter.

Quantities of physical interest

Expressions for drag force and heat transportation rate $\left(C_{fx},\ \mathrm{Nu}_x\right)$ in dimensional form are

$$C_{fx} = \frac{\tau_w}{U_w^2\rho_f}, \tag{14}$$

$$\mathrm{Nu}_x = -\frac{q_w x}{\left(T_\infty - T_w\right)k}, \tag{15}$$

in overhead expression $\left(q_w, \tau_w\right)$ characterizes the (wall heat flux, wall shear stress) which are given by

$$\tau_w = \mu\frac{\partial u}{\partial y}\left[\frac{1}{1 + \left(\Gamma\frac{\partial u}{\partial y}\right)^n}\right], \tag{16}$$

$$q_r = -\frac{16\sigma^{**}T_\infty^3}{3k^*}\frac{\partial T}{\partial y}. \tag{17}$$

Expressions of surface drag force and local Nusselt number in dimensionless form are given by

$$C_{fx}Re_x^{1/2} = \left[\frac{1}{1 + \left(\mathrm{Wef}''(0)\right)^n}\right]f''(0), \tag{18}$$

$$Nu_xRe_x^{-1/2} = -\left[1 + \frac{4}{3}R\right]\theta'(0), \tag{19}$$

where $Re_x = \frac{xU_w}{\nu}$ signifies local Reynolds number.

Analysis for entropy generation

Mathematical relation of entropy generation for cross liquid in dimensional form is defined as

$$S_G = \frac{k}{T_\infty^2}\left[(1 + \frac{16\sigma^*T_\infty^3}{3kk^*})\left(\frac{\partial T}{\partial y}\right)^2\right] + \frac{\mu}{T_\infty}\left(\frac{\partial u}{\partial y}\right)^2\left[\frac{1}{1 + \left(\Gamma\frac{\partial u}{\partial y}\right)^n}\right] + \frac{\sigma B_0^2u^2}{T_\infty} + \frac{\mathrm{RD}}{C_\infty}\left(\frac{\partial C}{\partial y}\right)^2 + \frac{\mathrm{RD}}{T_\infty}\left(\frac{\partial T}{\partial y}\frac{\partial C}{\partial y}\right). \tag{20}$$

The overhead relation in dimensionless is expressed as

$$N_G = \alpha_1\left[1 + \frac{4}{3}R\right]\theta'^2 + Br\left[\frac{1}{1 + \left(Wef''\right)^n}\right] f''^2 + MBrf'^2 + \frac{\alpha_2}{\alpha_1}L\phi'^2 + L\theta'\phi', \tag{21}$$

where $N_G = \frac{\nu T_\infty S_G}{\kappa c\,\Delta T}$ depicts the entropy generation rate, $Br = \frac{\mu U_w^2}{\kappa\,\Delta T}$ is the Brinkman number and $\alpha_2 = \frac{\Delta T}{T_\infty}$ is the dimensionless temperature ratio variable.

Mathematically, Bejan number is defined as

$$Be = \frac{\alpha_1\left[1+\frac{4}{3}R\right]\theta'^2 + \frac{\alpha_2}{\alpha_1}L\phi'^2 + L\theta'\phi'}{\alpha_1\left[1+\frac{4}{3}R\right]\theta'^2 + Br\left[\frac{1}{1+(We f'')^n}\right]f''^2 + MBrf'^2 + \frac{\alpha_2}{\alpha_1}L\phi'^2 + L\theta'\phi'}. \quad (22)$$

Authentication of our outcomes

Table 1 shows prepared to authenticate the accuracy our outcomes. These tables demonstrate comparison of heat transport rate for numerous estimations of Pr with , Wang (1989), Gorla and Sidawi (1994) and Hamad (2011). It is perceived that our outcomes are in outstanding agreement.

Results

Nonlinear system subjected to conditions (11–13) is numerically tackled by employing Bvp4c scheme. Significant features of emerging physical parameters such as radiation parameter (R), magnetic parameter (M), thermophoresis parameter N_t, local Weissenberg number (We), Buoyancy ratio parameter Nr, Brownian motion parameter (N_b), chemical reaction parameter (σ), mixed convection parameter (λ), Prandtl parameter (Pr), Eckert number (Ec), activation energy parameter (E), Schmidt number (Sc), entropy generation rate (N_G), Brinkman number (Br), dimensionless concentration ratio variable (α_2), dimensionless temperature ratio variable (α_1), and diffusive variable (L) on velocity $f'(\eta)$, temperature $\theta(\eta)$, concentration of nanomaterials $\phi(\eta)$, Bejan number (Br), and entropy generation (N_G) are examined in this section. Figures 1–21 show sketched to visualize the behavior of physical parameter. Figure 1 portrays the characteristics of We on f'. Here, f' deteriorates via larger We for shear thinning liquid. Features of f' for varying Nr are described in Fig. 2. Larger Nr yields an augmentation in cross-nanoliquid velocity. Characteristics f' for varying λ are reported in Fig. 3. Increment in λ intensifies f'. Physically, raise in λ yields more buoyancy forces due to which velocity of cross-liquid boosts. Impact of M against f' is considered in Fig. 4. Here, f' declines for higher estimation of M. Velocity of cross nanoliquid is much higher in case of hydrodynamic when compared to hydromagnetic situation. This behavior of cross nanoliquid for hydromagnetic situation occur, because augmentation in M creates strong Lorentz force. Figure 5 demonstrates the aspects of Ec for θ. Here, θ intensifies for larger Ec.

Table 1 Comparison of our results with outcomes reported by Wang (1989), Gorla and Sidawi (1994) and Hamad (2011) for ($We = 0$)

Pr	$-\theta(0)$			
	Wang (1989)	Gorla and Sidawi (1994)	Hamad (2011)	Present results ($We = 0$)
0.07	0.0656	0.0656	0.0656	0.065526
0.7	0.1691	0.1691	0.1691	0.164037
0.7	0.4539	0.4539	0.4539	0.4182299
2	0.9114	0.9114	0.9114	0.826827
7	1.8954	1.8954	1.8954	1.80433
20	3.3539	3.3539	3.3539	3.25603
70	6.4622	6.4622	6.4622	6.36662

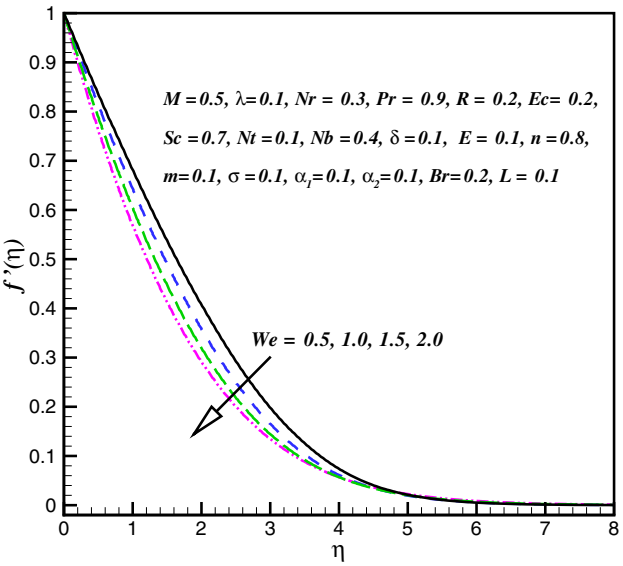

Fig. 1 f' impact for different We

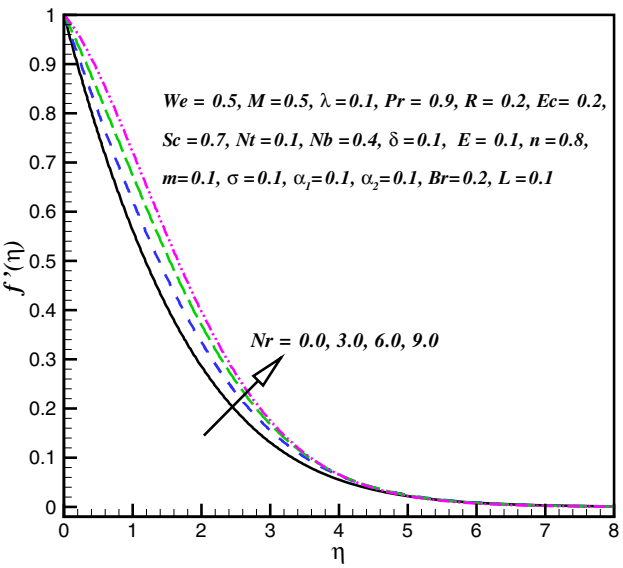

Fig. 2 f' impact for different Nr

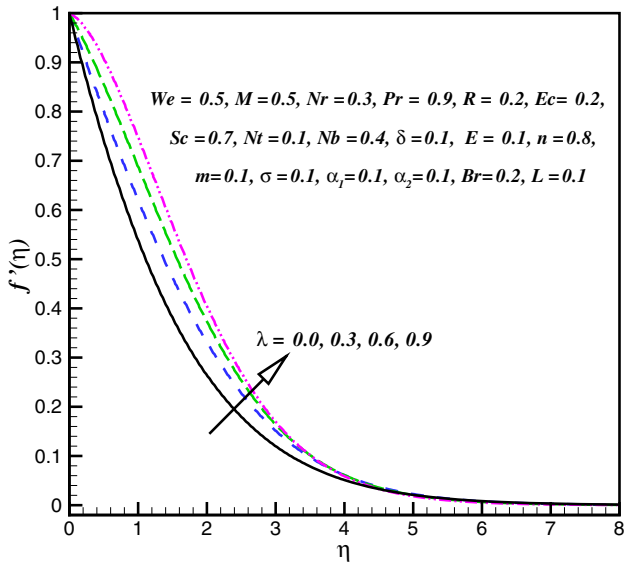

Fig. 3 f' impact for different λ

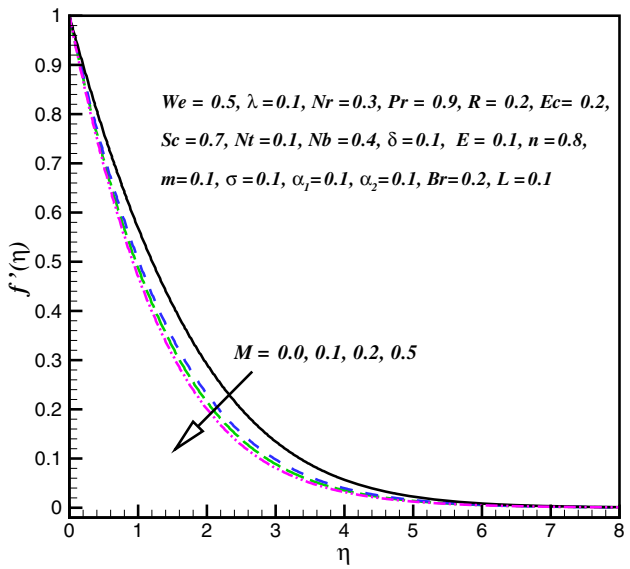

Fig. 4 f' impact for different M

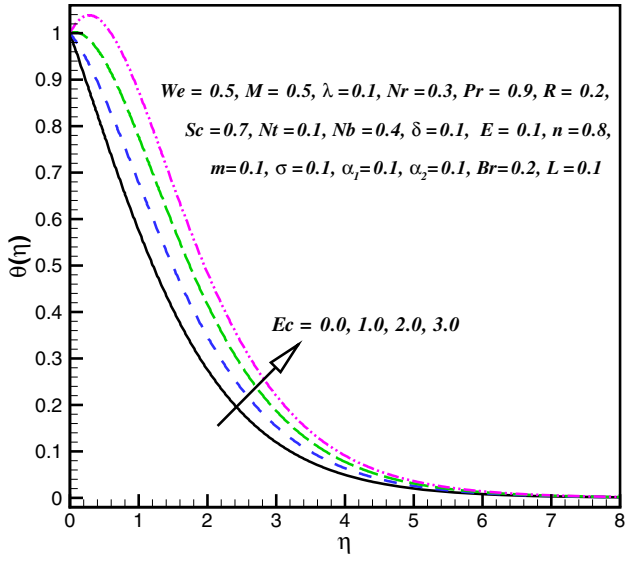

Fig. 5 θ impact for different Ec

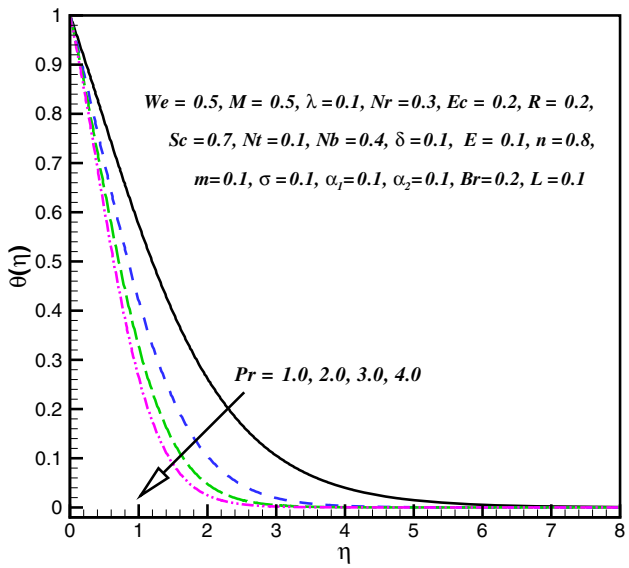

Fig. 6 θ impact for different Pr

Physically, greater values of Ec produce more heat due to temperature of cross-nanoliquid enhances. Attribute of Pr on θ is displayed in Fig. 6. Here, θ declines for greater Pr. Mathematical point of view Pr has inverse relation with thermal diffusivity. Therefore, greater Pr deteriorates significantly the temperature of cross nanoliquid. The curve of Nt for θ is presented in Fig. 7. Clearly, larger Nt yields higher θ. Actually, temperature difference between wall and at infinity rises due to temperature of cross-nanoliquid enhances. Nanofluid temperature upon R is illustrated through Fig. 8. An increment in R intensifies the nanoliquid temperature. Higher estimations of R produce more heat to working liquid. Figure 9 shows sketched to scrutinize the impact of σ on ϕ. Increment in σ deaccelerates the nanoparticles' volume fraction ϕ. Figure 10 portrays theaspect of E for nanoparticles volume fraction. It is perceived from achieved data that term $\exp\left(-\frac{E_a}{\kappa T}\right)$ deteriorates for greater values of E_a. Significance of Nt and Nb is emphasized in Figs. 11 and 12. For higher

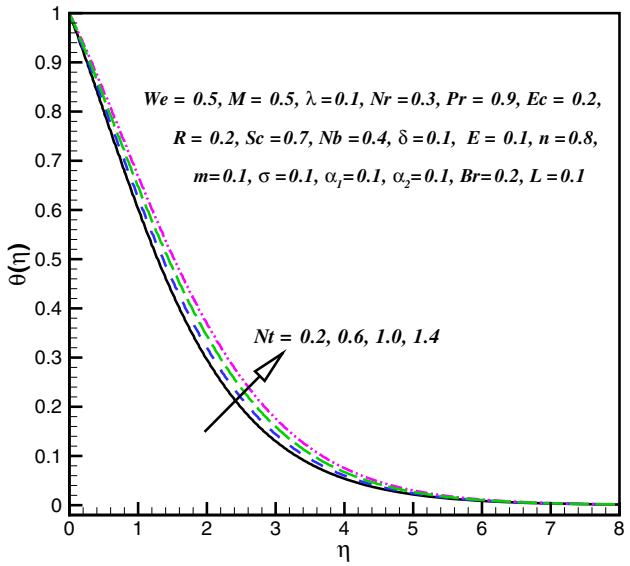

Fig. 7 θ impact for different Nt

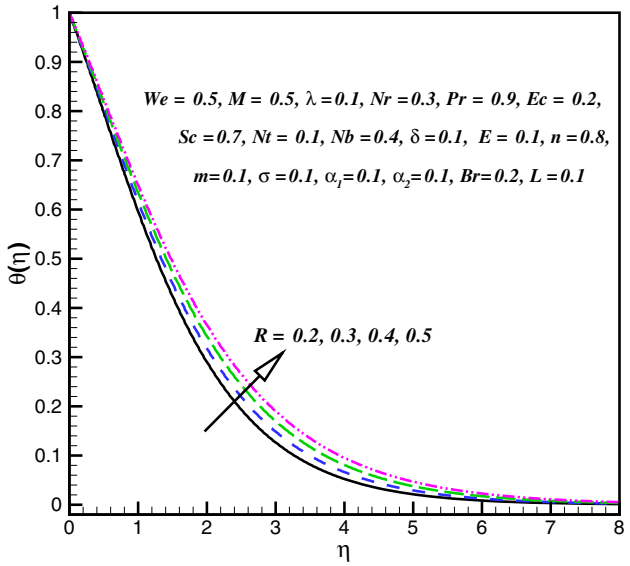

Fig. 8 θ impact for different R

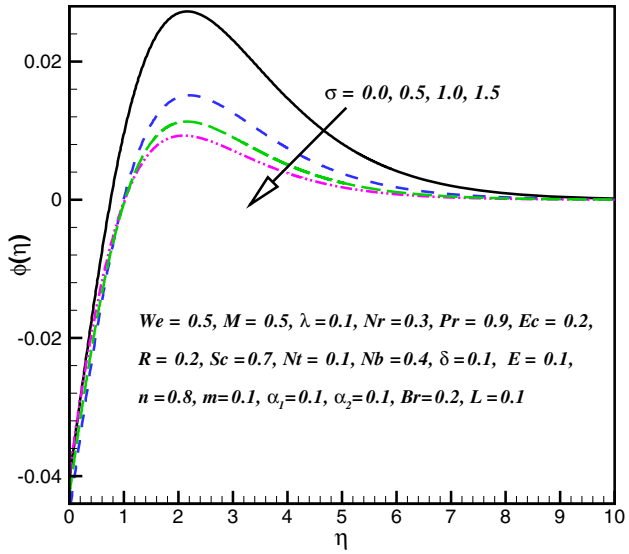

Fig. 9 ϕ impact for different σ

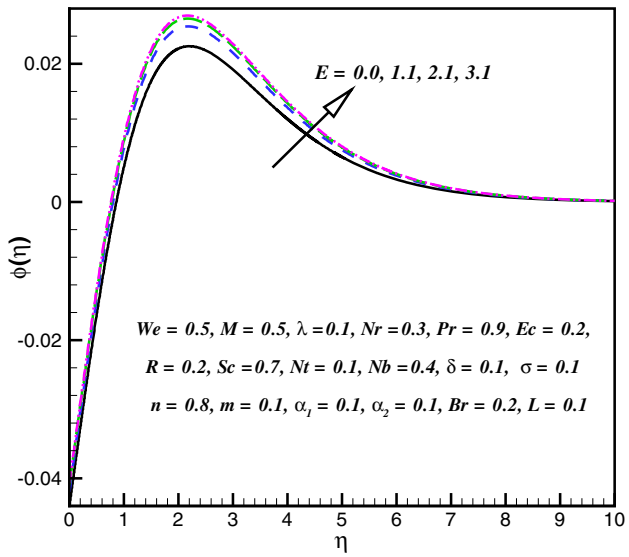

Fig. 10 ϕ impact for different E

estimation, Nt corresponds to enhancement in ϕ, while opposite behavior is captured for Nb. Actually, due to temperature difference between walls, nanoparticles are from higher temperature region to lower temperature reg ion.

Entropy generation rate and Bejan number

Figures 13 and 14 explain significant features of Br on N_G and Be. It is perceived that greater Br leads to an enrichment in the rate of entropy generation. Mathematically, Br has inverse relation to Be. Consequently, Be deteriorate, while opposite trend is detected for N_G. Behavior of L for rate of entropy generation N_G is disclosed through Fig. 15. This figure elaborates reduction N_G subjected to L. Figures 16 and 17 sketch to interpret the attribute of M for N_G and Be. Here, N_G intensifies and Be deteriorates subjected to higher M. Such a growth in N_G is perceived because resistance to motion of cross nanoliquid rises when M is enlarged. Figure 18 exhibits variation of α_1 versus N_G. Clearly, N_G intensifies subjected to higher α_1. Figure 19 describes α_2 influence on N_G. It is perceived from achieved data that N_G rises for larger α_2. Figures 20 and 21 sketch to demonstrate effect of R on N_G and Be. N_G and Be are augmented via larger R.

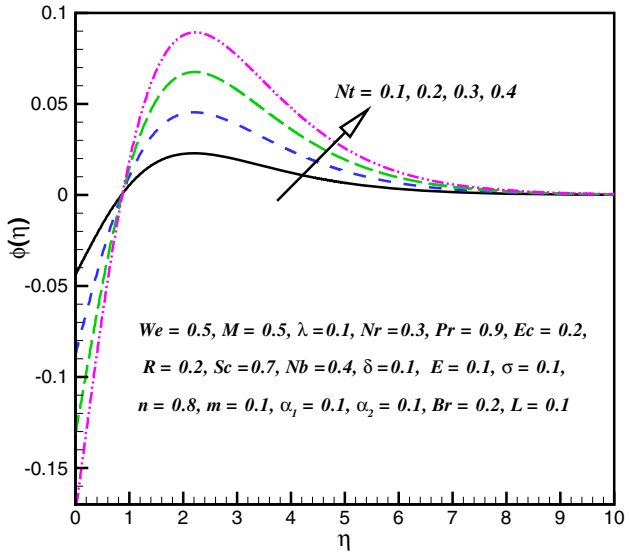

Fig. 11 ϕ impact for different N_t

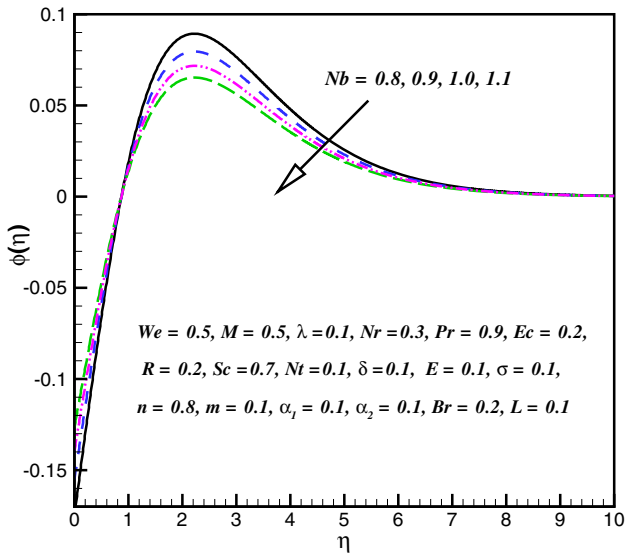

Fig. 12 ϕ impact for different N_b

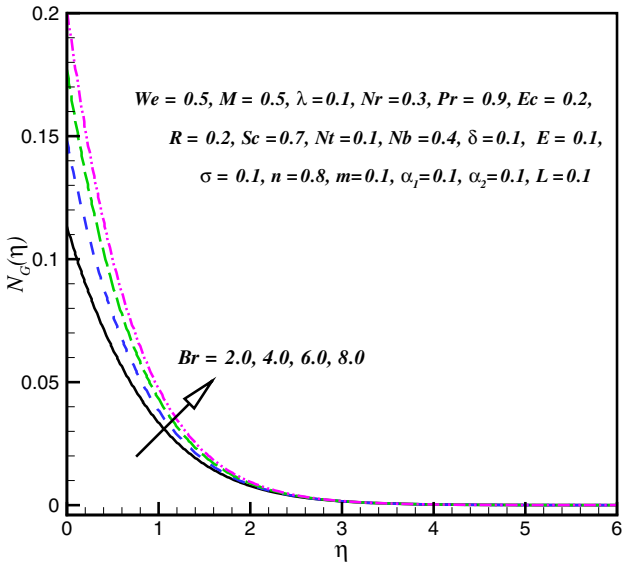

Fig. 13 N_G impact for different Br

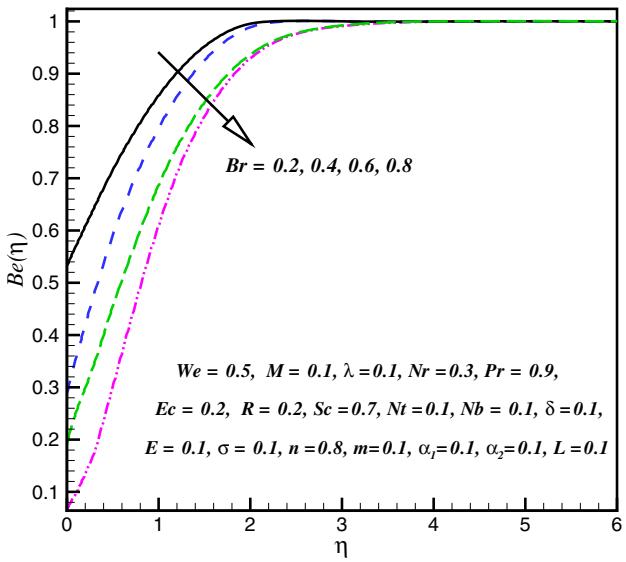

Fig. 14 Be impact for different Br

Characteristics of surface drag force and heat transfer rate

This subsection demonstrates the features of M, λ and We on surface drag force via Table 2. We perceived that surface drag force boosts via larger Nr for $n < 1$. Moreover, it is scrutinized that surface drag force decline via larger M, λ, and We for both $n < 1$ and $n > 1$. Table 3 elaborates the influence of numerous rheological parameters on heat transfer rate. Clearly, heat transfer rate rises for increments in Pr and R, while decays for higher Ec and N_t.

Conclusions

Here, mixed convective cross-nanoliquid flow containing magnetohydrodynamic (MHD) was scrutinized. Energy distribution of cross nanoliquid was investigated

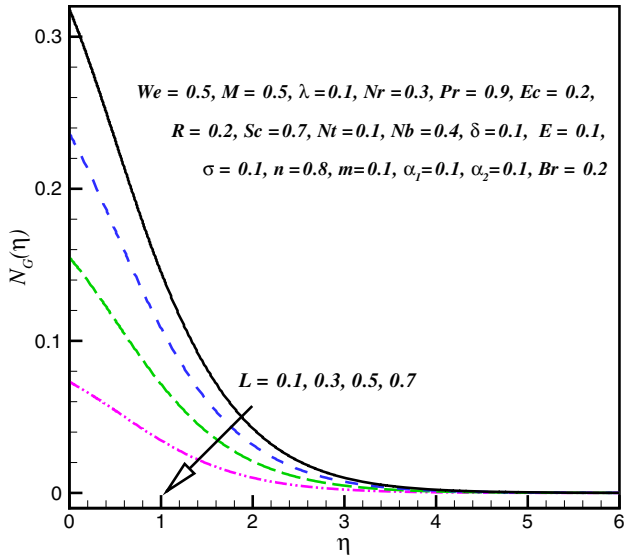

Fig. 15 N_G impact for different L

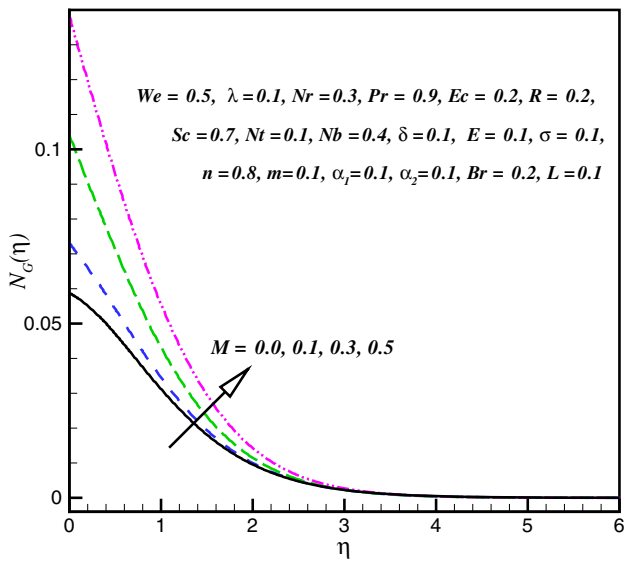

Fig. 16 N_G impact for different M

by considering Joule heating and radiation aspects. Significant outcomes prominent from whole analysis were as below.

- Increment in local Weissenberg number deteriorates cross-liquid velocity.

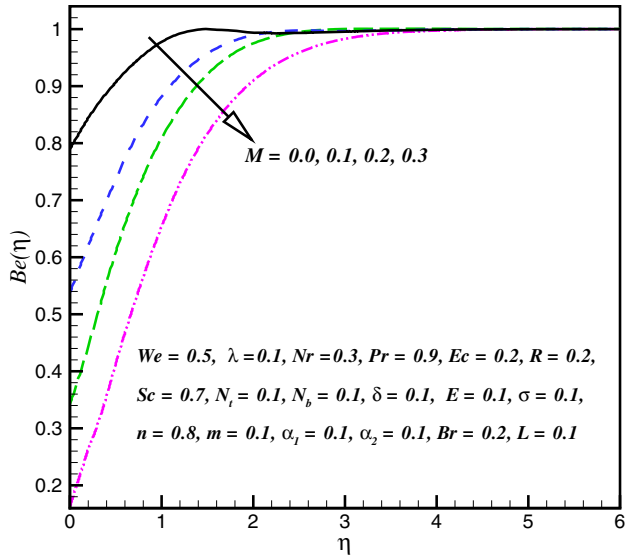

Fig. 17 *Be* impact for different M

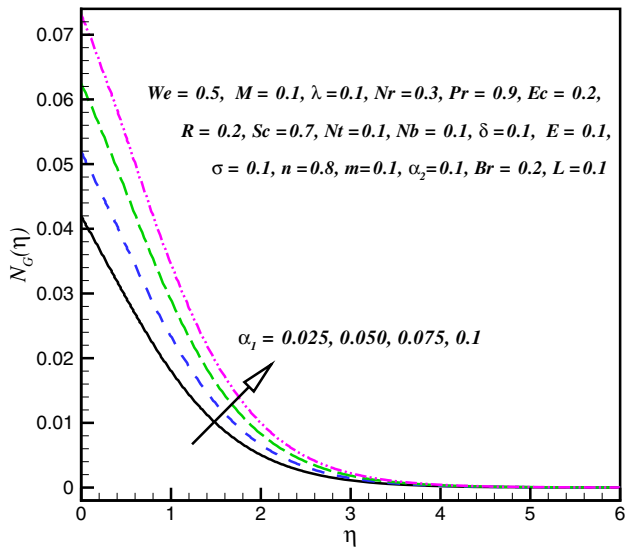

Fig. 18 N_G impact for different α_1

- Higher mixed convection parameter enriches the nanoliquid velocity.
- Larger radiation parameter intensifies the liquid temperature.
- Entropy generation boosts subjected to M, Br, R, α_1, and α_2; however, it diminishes when L is increased.
- Impact of M and R is reverse against Bejan number.

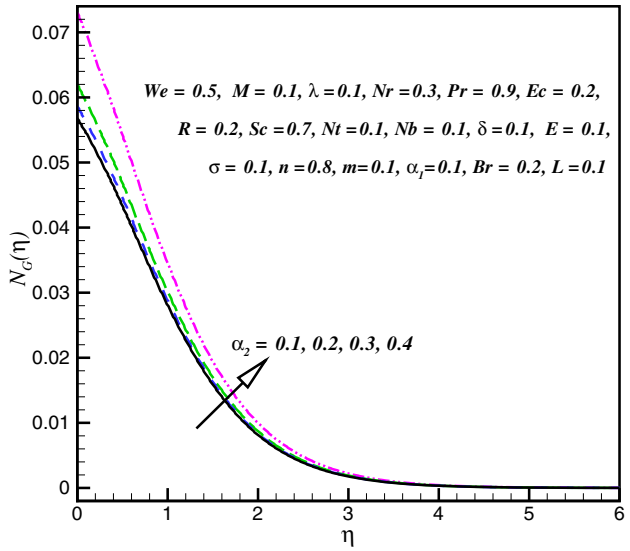

Fig. 19 N_G impact for different α_2.

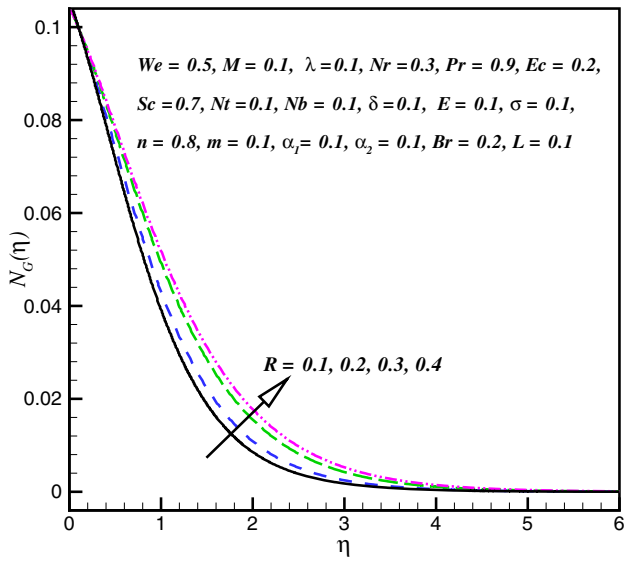

Fig. 20 N_G impact for different R

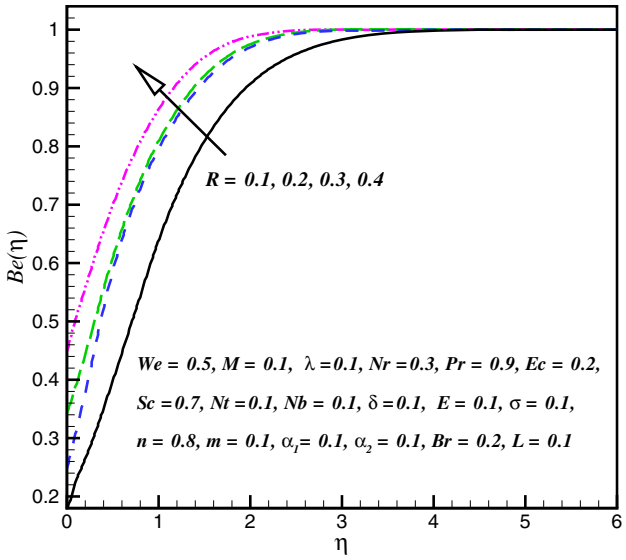

Fig. 21 *Be* impact for different *R*

Table 2 Surface drag force $C_{fx}Re_x^{1/2}$ via different estimations of *We*, λ, *Nr* and *M* when $\alpha_1 = \sigma = \alpha_2 = E = L = \delta = Nt = m = 0.1$, $Pr = 0.9$, $R = Ec = \mathrm{Br} = 0.2$, $\mathrm{Sc} = 0.7$, $Nb = 0.4$

$-Re^{1/2}C_{fx}$					
We	*M*	λ	Nr	$n = 0.8$	$n = 1.2$
0.2	–	–	–	0.7721269	0.8092971
0.4	–	–	–	0.7774658	0.8308007
0.6	–	–	–	0.7787053	0.8449733
–	0.5	–	–	0.6913445	0.7285802
–	0.7	–	–	0.6287607	0.6403177
–	0.9	–	–	0.4808132	0.4731329
–	–	0.2	–	0.4198645	0.4061171
–	–	0.5	–	0.2453616	0.2156822
–	–	0.8	–	0.06576118	0.03846451
–	–	–	0.3	0.07253961	0.0388256
–	–	–	0.4	0.07273982	0.0400191
–	–	–	0.5	0.07284708	0.04024486

Table 3 Heat transfer rate $Re^{-1/2}\,Nu_x$ via different estimations of Ec, Pr, We, Nt and R when $Nr = 0.3$, $Nb = 0.4$, $Sc = 0.7$, $m = \sigma = E = \delta = \lambda = 0.1$

$Nu_x Re_x^{-1/2}$					
Ec	Nt	Pr	R	$n = 0.5$	$n = 1.5$
0.0	–	–	–	0.654618	0.647758
0.2	–	–	–	0.595825	0.590746
0.3	–	–	–	0.566562	0.56238
–	0.1	–	–	0.582983	0.578339
–	0.3	–	–	0.572247	0.567674
–	0.5	–	–	0.56139	0.557107
–	–	1.0	–	0.621736	0.617283
–	–	1.3	–	0.721488	0.716412
–	–	1.7	–	0.837034	0.831459
–	–	–	0.4	0.646259	0.641688
–	–	–	0.5	0.669509	0.664755
–	–	–	0.6	0.691762	0.68672

References

Akbar NS, Khan ZH (2016) Effect of variable thermal conductivity and thermal radiation with CNTS suspended nanofluid over a stretching sheet with convective slip boundary conditions: numerical study. J Mol Liq 222:279–286

Ellahi R, Hassan M, Zeeshan A (2015) Shape effects of nanosize particles in Cu-H_2O nanofluid on entropy generation. Int J Heat Mass Transf 81:449–456

Gireesha BJ, Mahanthesh B, Thammanna GT, Sampathkumar PB (2018) Hall effects on dusty nanofluid two-phase transient flow past a stretching sheet using KVL model. J Mol Liq 256:139–147

Gorla RSR, Sidawi I (1994) Free convection on a vertical stretching surface with suction and blowing. Appl Sci Res 52:247–257

Hamad MAA (2011) Analytical solution of natural convection flow of a nanofluid over a linearly stretching sheet in the presence of magnetic field. Int Commun Heat Mass Transf 38:487–492

Hayat T, Rashid M, Imtiaz M, Alsaedi A (2017) MHD effects on a thermo-solutal stratied nanoáuid flow on an exponentially radiating stretching sheet. J Appl Mech Tech Phys 58:58. https://doi.org/10.1134/s0021894417020043

Hayat T, Kiyani MZ, Alsaedi A, Khan MI, Ahmad I (2018) Mixed convective three-dimensional flow of Williamson nanofluid subject to chemical reaction. Int J Heat Mass Transf 127:422–429

Irfan M, Khan M, Khan WA, Ayaz M (2018a) Modern development on the features of magnetic field and heat sink/source in Maxwell nanofluid subject to convective heat transport. Phys Lett A 382(30):1992–2002

Irfan M, Khan M, Khan WA (2018b) Behavior of stratifications and convective phenomena in mixed convection flow of 3D Carreau nanofluid with radiative heat flux. J Braz Soc Mech Sci Eng. https://doi.org/10.1007/s40430-018-1429-5

Irfan M, Khan M, Khan WA (2018c) Interaction between chemical species and generalized Fourier's law on 3D flow of Carreau fluid with variable thermal conductivity and heat sink/source: a numerical approach. Results Phys 10:107–117

Irfan M, Khan M, Khan WA, Ahmad L (2019a) Influence of binary chemical reaction with Arrhenius activation energy in MHD nonlinear radiative flow of unsteady Carreau nanofluid: dual solutions. Appl Phys A. https://doi.org/10.1007/s00339-019-2457-4

Irfan M, Khan M, Khan WA (2019b) Impact of homogeneous–heterogeneous reactions and non-Fourier heat flux theory in Oldroyd-B fluid with variable conductivity. J Braz Soc Mech Sci Eng 41:135. https://doi.org/10.1007/s40430-019-1619-9

Khan WA, Khan M (2014) Three-dimensional flow of an Oldroyd-B nanofluid towards stretching surface with heat generation/absorption. PLoS One 9(8):e10510

Khan M, Khan WA (2015) Forced convection analysis for generalized Burgers nanofluid flow over a stretching sheet. AIP Adv 5:107138. https://doi.org/10.1063/1.4935043

Khan M, Khan WA (2016a) MHD boundary layer flow of a power-law nanofluid with new mass flux condition. AIP Adv 6:025211. https://doi.org/10.1063/1.4942201

Khan M, Khan WA (2016b) Steady flow of Burgers nanofluid over a stretching surface with heat generation/absorption. J Braz Soc Mech Sci Eng. 38(8):2359–2367

Khan M, Khan WA, Alshomrani AS (2016a) Non-linear radiative flow of three-dimensional Burgers nanofluid with new mass flux effect. Int J Heat Mass Transf 101:570–576

Khan WA, Alshomrani AS, Khan M (2016b) Assessment on characteristics of heterogeneous-homogenous processes in three-dimensional flow of Burgers fluid. Results Phys 6:772–779

Khan WA, Irfan M, Khan M, Alshomrani AS, Alzahrani AK, Alghamdi MS (2017) Impact of chemical processes on magneto nanoparticle for the generalized Burgers fluid. J Mol Liq 234:201–208

Khan WA, Alshomrani AS, Alzahrani AK, Khan M, Irfan M (2018a) Impact of autocatalysis chemical reaction on nonlinear radiative heat transfer of unsteady three-dimensional Eyring–Powell magneto-nanofluid flow. Pramana 91:63. https://doi.org/10.1007/s12043-018-1634-x

Khan MI, Qayyum S, Hayat T, Khan MI, Alsaedi A, Khan TA (2018b) Entropy generation in radiative motion of tangent hyperbolic nanofluid in presence of activation energy and nonlinear mixed convection. Phys Lett A 382:2017–2026

Khan WA, Sultan F, Ali M, Shahzad M, Khan M, Irfan M (2019) Consequences of activation energy and binary chemical reaction for 3D flow of Cross-nanofluid with radiative heat transfer. J Braz Soc Mech Sci Eng. https://doi.org/10.1007/s40430-018-1482-0

Mahanthesh B, Gireesha BJ, Athira PR (2017) Radiated flow of chemically reacting nanoliquid with an induced magnetic field across a permeable vertical plate. Results Phys 7:2375–2383

Mahanthesh B, Gireesha BJ, Shehzad SA, Rauf A, Kumar PBS (2018) Nonlinear radiated MHD flow of nanoliquids due to a rotating disk with irregular heat source and heat flux condition. Phys B Condens Matt 537:98–104

Nematpour-Keshteli A, Sheikholeslami M (2019) Nanoparticle enhanced PCM applications for intensification of thermal performance in building: a review. J Mol Liq 274:516–533

Ramesh GK, Shehzad SA, Hayat T, Alsaedi A (2018) Activation energy and chemical reaction in Maxwell magneto-nanoliquid with passive control of nanoparticle volume fraction. J Braz Soc Mech Sci Eng. https://doi.org/10.1007/s40430-018-1353-8

Shahzad M, Sultan F, Haq I, Ali M, Khan WA (2019) C-matrix and invariants in chemical kinetics: a mathematical concept. Pramana 92:64. https://doi.org/10.1007/s12043-019-1723-5

Sheikholeslami M (2018a) Numerical approach for MHD Al_2O_3-water nanofluid transportation inside a permeable medium using innovative computer method. Comput Methods Appl Mech Eng. https://doi.org/10.1016/j.cma.2018.09.042

Sheikholeslami M (2018b) New computational approach for exergy and entropy analysis of nanofluid under the impact of Lorentz force through a porous media. Comput Methods Appl Mech Eng 25:22. https://doi.org/10.1016/j.cma.2018.09.044

Sheikholeslami M (2019a) New computational approach for exergy and entropy analysis of nanofluid under the impact of Lorentz

force through a porous media. Comput Methods Appl Mech Eng 344:319–333
Sheikholeslami M (2019b) Numerical approach for MHD Al_2O_3-water nanofluid transportation inside a permeable medium using innovative computer method. Comput Methods Appl Mech Eng 344:306–318
Sheikholeslami M, Mahian O (2019) Enhancement of PCM solidification using inorganic nanoparticles and an external magnetic field with application in energy storage systems. J Clean Prod 215:963–977
Sheikholeslami M, Rokni HB (2017) Numerical modeling of nanofluid natural convection in a semi annulus in existence of Lorentz force. Comput Methods Appl Mech Eng 317:419–430
Sheikholeslami M, Rokni HB (2018) Numerical simulation for impact of Coulomb force on nanofluid heat transfer in a porous enclosure in presence of thermal radiation. Int J Heat Mass Transf 118:823–831
Sheikholeslami M, Sadoughi MK (2018) Simulation of CuO-water nanofluid heat transfer enhancement in presence of melting surface. Int J Heat Mass Transf 116:909–919
Sheikholeslami M, Seyednezhad M (2018) Simulation of nanofluid flow and natural convection in a porous media under the influence of electric field using CVFEM. Int J Heat Mass Transf 120:772–781
Sheikholeslami M, Shamlooei M (2017) Fe_3O_4–H_2O nanofluid natural convection in presence of thermal radiation. Int J Hydrog Energy 42(9):5708–5718
Sheikholeslami M, Shehzad SA (2017) Magnetohydrodynamic nanofluid convective flow in a porous enclosure by means of LBM. Int J Heat Mass Transf 113:796–805
Sheikholeslami M, Shehzad SA (2018a) Simulation of water based nanofluid convective flow inside a porous enclosure via non-equilibrium model. Int J Heat Mass Transf 120:1200–1212
Sheikholeslami M, Shehzad SA (2018b) Numerical analysis of Fe_3O_4–H_2O nanofluid flow in permeable media under the effect of external magnetic source. Int J Heat Mass Transf 118:182–192
Sheikholeslami M, Bandpy MG, Ellahi R, Zeeshan A (2014) Simulation of MHD CuO-water nanofluid flow and convective heat transfer considering Lorentz forces. J Magn Mag Mater 369:69–80
Sheikholeslami M, Jafaryar M, Shafee A, Li Z (2018) Investigation of second law and hydrothermal behavior of nanofluid through a tube using passive methods. J Mol Liq 269:407–416
Sheikholeslami M, Rizwan-ul H, Shafee A, Li Z (2019a) Heat transfer behavior of nanoparticle enhanced PCM solidification through an enclosure with V shaped fins. Int J Heat Mass Transf 130:1322–1342
Sheikholeslami M, Gerdroodbary MB, Moradi R, Shafee A, Li Z (2019b) Application of Neural Network for estimation of heat transfer treatment of Al_2O_3-H_2O nanofluid through a channel. Comput Methods Appl Mech Eng 344:1–12
Sohail A, Khan WA, Khan M, Shah SIA (2017) Consequences of non-Fourier's heat conduction relation and chemical processes for viscoelastic liquid. Results Phys 7:3281–3286
Sulochana C, Ashwinkumar GP, Sandeep N (2017) Joule heating effect on a continuously moving thin needle in MHD Sakiadis flow with thermophoresis and Brownian moment. Eur Phys J Plus. https://doi.org/10.1140/epjp/i2017-11633-3
Wang CY (1989) Free convection on a vertical stretching surface. J Appl Math Mech (ZAMM) 69:418–420
Waqas M, Farooq M, Khan MI, Alsaedi A, Hayat T, Yasmeen T (2016) Magnetohydrodynamic (MHD) mixed convection flow of micropolar liquid due to nonlinear stretched sheet with convective condition. Int J Heat Mass Transf 102:766–772